Dedicated to Academician Aureliu Sandulescu's 80th Anniversary

FRpnQRPA APPROACH WITH THE GAUGE SYMMETRY RESTORED. APPLICATION FOR THE $2\nu\beta\beta$ DECAY

A. A. RADUTA[1,2]

[1]Department of Theoretical Physics,
"Horia Hulubei" National Institute for Physics and Nuclear Engineering,
Reactorului 30, RO-077125, POB-MG6, Măgurele-Bucharest, Romania
[2]Academy of Romanian Scientists, 54 Splaiul Independentei, Bucharest 050094, Romania
Email: raduta@nipne.ro

Received September 30, 2011

A many body Hamiltonian involving the mean field for a projected spherical single particle basis, the pairing interactions for alike nucleons, a repulsive dipole-dipole proton-neutron interaction in the particle-hole (ph) channel and an attractive dipole-pairing interaction is treated by a gauge restored and fully renormalized proton-neutron quasiparticle random phase approximation ($GRFRpnQRPA$) formalism. The resulting wave functions and energies for the mother and the daughter nuclei are used to calculate the $2\nu\beta\beta$ decay rate and the process half life for the emitters: ^{48}Ca, ^{76}Ge, ^{82}Se, ^{96}Zr, ^{100}Mo, ^{104}Ru, ^{110}Pd, ^{116}Cd, ^{128,130}Te, ^{148,150}Nd, ^{154}Sm, and ^{160}Gd. The results of our calculations are compared with the corresponding experimental data as well as with those obtained through other methods. The Ikeda sum rule (ISR) is obeyed.

Key words: Proton-neutron interaction, double beta decay, Ikeda sum rule, beta minus and beta plus strengths, transition amplitude, half life, total strength.

1. INTRODUCTION

The $2\nu\beta\beta$ process is interesting by its own but is also very attractive because it constitutes a test for the nuclear matrix elements (m.e.) which are used for the process of $0\nu\beta\beta$ decay. The discovery of this process may provide an answer to the fundamental question, whether neutrino is a Majorana or a Dirac particle. The subject development is described by several review papers [1–7]. The present paper refers to the $2\nu\beta\beta$ process, which is conceived as consisting of two consecutive and virtual single β^- decays. The formalism yielding closest results to the experimental data is the proton-neutron random phase approximation ($pnQRPA$) which includes the particle-hole (ph) and particle-particle (pp) as independent two body interactions. The second leg of the $2\nu\beta\beta$ process is very sensitive to changing the relative strength of the later interaction, denoted hereafter by g_{pp}. It is worth mentioning that the ph interaction is repulsive while the pp one is attractive. Consequently, there is a critical value of g_{pp} for which the first root of the $pnQRPA$ equation vanishes. Actually, this is the signal that the $pnQRPA$ approach is no longer valid. Moreover, the g_{pp} value which corresponds to a transition amplitude which agrees with the corresponding experimental data is close to the mentioned critical value. That means that the result is not stable to adding corrections to the RPA picture. An improvement for the $pnQRPA$ was achieved by one of us (AAR), in collaboration, in Refs. [8, 9], by using a boson expansion (BE) procedure. Another procedure, proposed in Ref. [10], renormalizes the dipole two quasiparticle operators by replacing the scalar components of their commutators with their average values. Such a renormalization is, however, inconsistently achieved since the scattering operators do not participate at the renormalization process. This lack of consistency was removed in Refs. [11, 12] where a fully renormalized $pnQRPA$ ($FRpnQRPA$) is proposed.

Unfortunately, all higher pnQRPA procedures mentioned above have the common drawback of violating the Ikeda sum rule (ISR) by an amount of about 20-30% [13]. It is believed that such a violation is caused by the gauge symmetry breaking. Consequently, a method of restoring this symmetry was formulated by two of us (A. A. R. and C. M. R.) in Ref. [14].

Recently [15, 16], the results of Ref. [14] were improved in two respects: a) aiming at providing a unitary description of the process for the situations when the involved nuclei are spherical or deformed, here we use the projected spherical single particle basis defined in Ref. [17] and used for double beta decay in Refs. [18, 19]; b) the space of proton-neutron dipole configurations is split in three subspaces, one being associated to the single β^- decay, one to the single β^+ process, and one spanned by the unphysical states. A set of $GRFRpnQRPA$ equations is written down in the first two subspaces mentioned above, by linearizing the equations of motion of the basic transition operators corresponding to the two coupled processes.

In the present paper we apply the equations derived by the $GRFRpnQRPA$ for the $2\nu\beta\beta$ processes ^{48}Ca$\to^{48}$Ti, ^{76}Ge$\to^{76}$Se, ^{82}Se $\to^{82}$Kr and ^{96}Zr $\to^{96}$Mo, ^{104}Ru $\to^{104}$Pd, ^{110}Pd $\to^{110}$Cd, ^{128}Te $\to^{128}$Xe, ^{130}Te $\to^{130}$Xe, ^{148}Nd $\to^{148}$Sm, ^{150}Nd $\to^{150}$Sm, ^{154}Sm $\to^{154}$Gd and ^{160}Gd $\to^{160}$Dy. New arguments supporting the formalism are given. Moreover due to the specific experimental available data a new procedure for fixing the strengths of the two body pn interactions is presented. A detailed comparison to other models aiming at being realistic and at the same time at fulfilling the Ikeda sum rule is mentioned.

Results are described according to the following plan. The model Hamiltonian is given in Section II where, also, The FRpnQRPA approach is shortly discussed. The projected gauge of $FRpnQRPA$ ($GRFRpnQRPA$) is the objective of Section III. The Gamow-Teller (GT) amplitude for the $2\nu\beta\beta$ process is given in Section IV. Numerical applications are shown in Section IV, while the final conclusions are drawn in Section V.

2. THE MODEL HAMILTONIAN

In Ref. [17], one of us, (A.A.R., in collaboration), introduced an angular momentum projected single particle basis which seems to be appropriate for the description of the single particle motion in a deformed mean field generated by the particle-core interaction. This single particle basis has been used to study the collective M1 states in deformed nuclei [17, 20, 21] as well as the rate of double beta process [18, 22, 23]. The basis is defined by projecting out the angular momentum from a product state:

$$\Phi^{IM}_{nlj}(d) = \mathcal{N}^{I}_{nlj} P^{I}_{MI}[|nljI\rangle \Psi_g] \equiv \mathcal{N}^{I}_{nlj} \Psi^{IM}_{nlj}(d), \tag{1}$$

with $|nljI\rangle$ denoting a spherical shell model state and Ψ_g an axially symmetric deformed function which is the coherent state defined with the zeroth component of a quadrupole boson operator:

$$\Psi_g = exp[d(b^{+}_{20} - b_{20})]|0\rangle_b. \tag{2}$$

The quadrupole boson operators are related with the quadrupole shape coordinates by the canonical transformation:

$$\alpha_{2\mu} = \frac{1}{k\sqrt{2}}\left(b^{\dagger}_{2\mu} + (-)^{\mu} b_{2,-\mu}\right), \tag{3}$$

where k is an arbitrary C number.

The projected states defined above can be used as single particle basis, as proved in our previous publications. To the projected spherical basis, one associates a set of deformed single particle energies, $\epsilon^{I}_{nlj}(d)$, defined as average values of a single particle-core Hamiltonian. The deformation dependence of the new single particle energies is similar to that shown by the Nilsson model [24] energies. Therefore, the average values ϵ^{I}_{nlj} may be viewed as approximate single particle energies in deformed Nilsson orbits [24]. We may account for the deviations from the exact eigenvalues by considering, at a later stage when a specific treatment of the many body system is performed, the exact matrix elements of the two body interaction.

We suppose that the states describing the nuclei involved in a $2\nu\beta\beta$ process are described by a many body Hamiltonian which may be written in the projected spherical basis as:

$$H = \sum_{\tau,\alpha,I,M} \frac{2}{2I+1}(\epsilon_{\tau\alpha I} - \lambda_{\tau\alpha}) c^{\dagger}_{\tau\alpha IM} c_{\tau\alpha IM} - \sum_{\tau,\alpha,I,I'} \frac{G_\tau}{4} P^{\dagger}_{\tau\alpha I} P_{\tau\alpha I'}$$
$$+ 2\chi \sum_{pn;p'n';\mu} \beta^{-}_{\mu}(pn)\beta^{+}_{-\mu}(p'n')(-)^{\mu} - 2\chi_1 \sum_{pn;p'n';\mu} P^{-}_{\mu}(pn)P^{+}_{-\mu}(p'n')(-)^{\mu}, \tag{4}$$

where $c^{\dagger}_{\tau\alpha IM}(c_{\tau\alpha IM})$ denotes the creation (annihilation) operator of one nucleon of the type $\tau(=p,n)$ in the state Φ_α^{IM}, with α being an abbreviation for the set of quantum numbers nlj. The Hamiltonian H contains the mean field term, the pairing interactions for alike nucleons whose strengths are denoted by G_τ and the Gamow-Teller dipole-dipole interaction in the ph and pp channels, characterized by the strengths χ and χ_1, respectively.

In order to simplify the notations, hereafter the set of quantum numbers $\alpha(= nlj)$ will be omitted. Note that the two body interactions are separable, with the factors defined by the following expressions:

$$\begin{aligned}
P^\dagger_{\tau I} &= \sum_M \frac{2}{2I+1} c^\dagger_{\tau IM} c^\dagger_{\widetilde{\tau IM}}, \\
\beta^-_\mu(pn) &= \sum_{M,M'} \frac{\sqrt{2}}{\hat{I}} \langle pIM|\sigma_\mu|nI'M'\rangle \frac{\sqrt{2}}{\hat{I'}} c^\dagger_{pIM} c_{nI'M'}, \\
P^-_{1\mu}(pn) &= \sum_{M,M'} \frac{\sqrt{2}}{\hat{I}} \langle pIM|\sigma_\mu|nI'M'\rangle \frac{\sqrt{2}}{\hat{I'}} c^\dagger_{pIM} c^\dagger_{\widetilde{nI'M'}}.
\end{aligned} \tag{5}$$

The other operators from Eq.(4) can be obtained from the above expressions, by Hermitian conjugation.

In the quasiparticle representation, defined by the Bogoliubov-Valatin transformation:

$$a^\dagger_{\tau IM} = U_{\tau I} c^\dagger_{\tau IM} - s_{IM} V_{\tau I} c_{\tau I-M}, s_{IM} = (-)^{I-M},\ \tau = p,n,\ U^2_{\tau I} + V^2_{\tau I} = 1, \tag{6}$$

the first two terms of H are replaced by the independent quasiparticles term, $\sum E_{\tau I}$ $a^\dagger_{\tau IM} a_{\tau IM}$, while the ph and pp interactions are expressed in terms of the dipole two qp and the qp dipole density operators:

$$\begin{aligned}
A^\dagger_{1\mu}(pn) &= \sum C^{I_p\, I_n\, 1}_{m_p\, m_n\, \mu} a^\dagger_{pI_pm_p} a^\dagger_{nI_nm_n},\ A_{1\mu}(pn) = \left(A^\dagger_{1\mu}(pn)\right)^\dagger, \\
B^\dagger_{1\mu}(pn) &= \sum C^{I_p\, I_n\, 1}_{m_p\, -m_n\, \mu} a^\dagger_{pj_pm_p} a_{nI_nm_n} (-)^{I_n-m_n},\ B_{1\mu}(pn) = \left(B^\dagger_{1\mu}(pn)\right)^\dagger,
\end{aligned} \tag{7}$$

As shown in [11], all these operators can be renormalized by making use of the commutation equations:

$$\begin{aligned}
\left[A_{1\mu}(k), A^\dagger_{1\mu'}(k')\right] &\approx \delta_{k,k'}\delta_{\mu,\mu'} \left[1 - \frac{\hat{N}_n}{\hat{I}^2_n} - \frac{\hat{N}_p}{\hat{I}^2_p}\right], \\
\left[B^\dagger_{1\mu}(k), A^\dagger_{1\mu'}(k')\right] &\approx \left[B^\dagger_{1\mu}(k), A_{1\mu'}(k')\right] \approx 0, \\
\left[B_{1\mu}(k), B^\dagger_{1\mu'}(k')\right] &\approx \delta_{k,k'}\delta_{\mu,\mu'} \left[\frac{\hat{N}_n}{\hat{I}^2_n} - \frac{\hat{N}_p}{\hat{I}^2_p}\right],\ k = (I_p, I_n).
\end{aligned} \tag{8}$$

with $\hat{N}_\tau$ denoting the quasiparticle number operator of type τ(=p,n). Indeed, denoting by $C^{(1)}_{I_p,I_n}$ and $C^{(2)}_{I_p,I_n}$ the averages of the right hand sides of (8) with the renormalized $pnQRPA$ vacuum state, the renormalized operators defined as

$$\bar{A}_{1\mu}(k) = \frac{1}{\sqrt{C^{(1)}_k}} A_{1\mu},\ \bar{B}_{1\mu}(k) = \frac{1}{\sqrt{|C^{(2)}_k|}} B_{1\mu}, \tag{9}$$

obey the boson-like commutation relations:

$$\begin{aligned}\left[\bar{A}_{1\mu}(k), \bar{A}^\dagger_{1\mu'}(k')\right] &= \delta_{k,k'}\delta_{\mu,\mu'},\\ \left[\bar{B}_{1\mu}(k), \bar{B}^\dagger_{1\mu'}(k')\right] &= \delta_{k,k'}\delta_{\mu,\mu'} f_k,\ \ f_k = sign(C^{(2)}_k).\end{aligned} \tag{10}$$

Further, these operators are used to define the phonon operator:

$$C^\dagger_{1\mu}=\sum_k \left[X(k)\bar{A}^\dagger_{1\mu}(k)+Z(k)\bar{D}^\dagger_{1\mu}(k)-Y(k)\bar{A}_{1-\mu}(k)(-)^{1-\mu}-W(k)\bar{D}_{1-\mu}(k)(-)^{1-\mu}\right], \tag{11}$$

where $\bar{D}^\dagger_{1\mu}(k)$ is equal to $\bar{B}^\dagger_{1\mu'}(k')$ or $\bar{B}_{1\mu}(k)$ depending on whether f_k is + or -. The phonon amplitudes are determined by the equations:

$$\left[H, C^\dagger_{1\mu}\right] = \omega C^\dagger_{1\mu},\ \ \left[C_{1\mu}, C^\dagger_{1\mu'}\right] = \delta_{\mu\mu'}. \tag{12}$$

Interesting properties for these equations and their solutions were discussed in our previous publications [11, 12]. The formalism defined above was named as Fully Renormalized proton-neutron Quasiparticle Random Phase Approximation (*FRpn-QRPA*).

3. GAUGE PROJECTION OF THE FULLY RENORMALIZED PNQRPA

The ground state of a (N,Z) nucleus can be excited by the phonon operator, defined above, to a state which is a superposition of components describing the neighboring nuclei $(N-1,Z+1),(N+1,Z-1),(N+1,Z+1),(N-1,Z-1)$. The first two components conserve the total number of nucleons (N+Z) but violate the third component of isospin, T_3. By contrast, the last two components violate the total number of nucleons but preserve T_3. Actually, the last two components are those which contribute to the ISR violation. However, one can construct linear combinations of the basic operators $A^\dagger, A, B^\dagger, B$ which excite the nucleus (N,Z) to the nuclei $(N-1,Z+1),(N+1,Z-1),(N+1,Z+1),(N-1,Z-1)$, respectively. These operators are:

$$\begin{aligned}\mathcal{A}^\dagger_{1\mu}(pn) &= U_pV_nA^\dagger_{1\mu}(pn)+U_nV_pA_{1,-\mu}(pn)(-)^{1-\mu}+U_pU_nB^\dagger_{1\mu}(pn)-V_pV_nB_{1,-\mu}(pn)(-)^{1-\mu},\\ \mathcal{A}_{1\mu}(pn) &= U_pV_nA_{1\mu}(pn)+U_nV_pA^\dagger_{1,-\mu}(pn)(-)^{1-\mu}+U_pU_nB_{1\mu}(pn)-V_pV_nB^\dagger_{1,-\mu}(pn)(-)^{1-\mu},\\ \mathbf{A}^\dagger_{1\mu}(pn) &= U_pU_nA^\dagger_{1\mu}(pn)-V_pV_nA_{1,-\mu}(pn)(-)^{1-\mu}-U_pV_nB^\dagger_{1\mu}(pn)-V_pU_nB_{1,-\mu}(pn)(-)^{1-\mu},\\ \mathbf{A}_{1\mu}(pn) &= U_pU_nA_{1\mu}(pn)-V_pV_nA^\dagger_{1,-\mu}(pn)(-)^{1-\mu}-U_pV_nB_{1\mu}(pn)-V_pU_nB^\dagger_{1,-\mu}(pn)(-)^{1-\mu}.\end{aligned}$$

Indeed, in the particle representation these operators have the expressions:

$$\begin{aligned} \mathcal{A}^{\dagger}_{1\mu}(pn) &= -\left[c^{\dagger}_{p}c_{\widetilde{n}}\right]_{1\mu}, \quad \mathcal{A}_{1\mu}(pn) = -\left[c^{\dagger}_{p}c_{\widetilde{n}}\right]^{\dagger}_{1\mu}, \\ \mathbf{A}^{\dagger}_{1\mu}(pn) &= \left[c^{\dagger}_{p}c^{\dagger}_{n}\right]_{1\mu}, \quad \mathbf{A}_{1\mu}(pn) = \left[c^{\dagger}_{p}c^{\dagger}_{n}\right]^{\dagger}_{1\mu}. \end{aligned} \tag{13}$$

Thus, the operators from the first row excite the nucleus (N,Z) to the nuclei (N-1,Z+1) and (N+1,Z-1) respectively, while the operators $\mathbf{A}^{\dagger}_{1\mu}(pn)$ and $\mathbf{A}_{1\mu}(pn)$ bring (N,Z) to (N+1,Z+1) and (N-1,Z-1), respectively. In terms of the new operators, the many body Hamiltonian is:

$$\begin{aligned} H &= \sum_{\tau jm} E_{\tau j} a^{\dagger}_{\tau jm} a_{\tau jm} + 2\chi \sum_{pn,p'n';\mu} \sigma_{pn;p'n'} \mathcal{A}^{\dagger}_{1\mu}(pn)\mathcal{A}_{1\mu}(p'n') \\ &- 2\chi_1 \sum_{pn,p'n';\mu} \sigma_{pn;p'n'} \mathbf{A}^{\dagger}_{1\mu}(pn)\mathbf{A}_{1\mu}(p'n'), \\ \sigma_{pn;p'n'} &= \frac{2}{3\hat{I}_n\hat{I}_{n'}} \langle I_p||\sigma||I_n\rangle\langle I_{p'}||\sigma||I_{n'}\rangle, \end{aligned} \tag{14}$$

where $E_{\tau I}$ denotes the quasiparticle energy.

At this stage we have to explain why the pp interaction is not effective, i.e. does not contribute at all within our approach. Indeed, within the gauge preserved picture the operators $\mathcal{A}_{1\mu}$ and $\mathbf{A}^{\dagger}_{1\mu}$ commute with each other. Consequently, the gauge projected phonon operator cannot comprise terms like $\mathbf{A}^{\dagger}_{1\mu}$ since they violate the total number of nucleons.

Indeed, if the mentioned commutator would be different from zero, but equal to the average of its scalar part with the new vacuum state, then the equations of motion for the operators $\mathcal{A}_{1\mu}$ and $\mathcal{A}^{\dagger}_{1\mu}$ would be linear not only in the nucleon number conserving operators, but also in those which do not conserve the total number operator. In order that the equations of motion constitute a closed algebra, we have to add the equations corresponding to the number non-conserving operators. Consequently, the phonon operator is a linear combination of both nucleon number conserving and non-conserving terms. It is conspicuous now that in order to conserve the nucleon total number it is necessary to accept that the operators $\mathcal{A}_{1\mu}$ and $\mathbf{A}^{\dagger}_{1\mu}$ commute with each other. In this context the *pp* interaction is becoming inefficient for properties described by gauge preserving wave functions and therefore we have to ignore it. In this respect our formalism contrasts the picture of Ref. [48] where the phonon operator is commuting with the nucleon total number operator and at a time the pp interaction contributes to the renormalized $pnQRPA$ equations.

However, aiming at a quantitative description of the double beta process, the presence of an attractive proton-neutron interaction is necessary. Due to this reason we replace the *pp* interaction, which is ineffective anyway, with a dipole-pairing interaction:

$$\Delta H = -X_{dp} \sum_{\substack{pn;p' \\ n';\mu}} \left(\beta^{-}_{\mu}(pn)\beta^{-}_{-\mu}(p'n') + \beta^{+}_{-\mu}(p'n')\beta^{+}_{\mu}(pn)\right)(-1)^{1-\mu}. \tag{15}$$

We remark that the two terms of ΔH are changing the charge by +2 and -2 units respectively, and therefore one may think that it is not justified within the meson-dynamic theory of nuclear forces. That is not true, having in mind the isospin charge independence property of the nuclear forces. Also, we note that ΔH is Hermitian and invariant to rotation. This Hamiltonian should be looked at as an effective Hamiltonian in the same manner as the standard pairing Hamiltonian is. Indeed, within the BCS approximation the initial pairing Hamiltonian is replaced by an effective one $\Delta(c^{\dagger}c^{\dagger})_0 + \Delta^{*}(cc)_0$, with $c^{\dagger}$ (c) denoting the single particle creation (annihilation) operator and Δ the energy gap. This Hamiltonian also does not preserve the charge, but this is consistent with the trial variational state $|BCS\rangle$ which is a mixture of components with different even number of particles. In the present case the $pnQRPA$ state is built on the top of the BCS ground state which is a product of the BCS states for protons and neutrons respectively, which results in obtaining a linear superposition of components with different isospin third component, T_3. Of course, at the BCS level T_3 is preserved in the average. Therefore, in the quasiparticle picture the condition that the Hamiltonian commutes separately with the proton and neutron number operators is anyway not fulfilled by any of the composing terms from the model Hamiltonian. Note that ΔH commutes with the total number of nucleons and preserves this feature after the linearizing procedure is performed, contributing to the equations of motion of the basic operators with the gauge restored. Concerning the T_3 symmetry let us denote by $\mathcal{N}_{\tau}$ the τ (=p,n) particle number operators respectively, and calculate the commutator:

$$[\Delta H, \mathcal{N}_p - \mathcal{N}_n] = 4X_{dp} \sum_{\substack{pn;p' \\ n';\mu}} \left(\beta^{-}_{\mu}(pn)\beta^{-}_{-\mu}(p'n') - \beta^{+}_{-\mu}(p'n')\beta^{+}_{\mu}(pn)\right)(-1)^{1-\mu}. \tag{16}$$

Note that the right hand side of the above equation is an anti-Hermitian operator. Consequently, its average value with any state is vanishing. In particular it is vanishing if the chosen state is the BCS ground state or the vacuum state of the $GPFRpnQRPA$ phonon operator. Concluding, in the present formalism the third isospin component is conserved in the average. Clearly this happens since while one term of ΔH is increasing the charge by two units the other term is decreasing it by the same amount. Note that this isospin non-conserving term shows up even at the level of the standard $pnQRPA$. Indeed within this formalism the two-body interaction is approximated by any linear combination of the operators

$$A^{\dagger}_{1\mu}(pn)A_{1\mu}(pn), \quad (-1)^{1-\mu}\left(A^{\dagger}_{1\mu}(pn)A^{\dagger}_{1-\mu}(pn)+A_{1,-\mu}(pn)A_{1\mu}(pn)\right). \quad (17)$$

Writing these terms in the particle representation one finds that the effective two-body interaction comprises, among other terms, a term which is proportional to ΔH. Therefore in a formalism using approximations which violates the T_3 symmetry, the use of a Hamiltonian ΔH which is not preserving the T_3 component does not produce a special inconsistency.

Writing the model Hamiltonian in the quasiparticle representation, one obtains:

$$H=\sum_{\tau jm}E_{\tau j}a^{\dagger}_{\tau jm}a_{\tau jm}+2\chi\sum_{pn,p'n';\mu}\sigma_{pn;p'n'}\mathcal{A}^{\dagger}_{1\mu}(pn)\mathcal{A}_{1\mu}(p'n')$$
$$-X_{dp}\sum_{pn;p'n';\mu}\sigma_{pn;p'n'}\left(\mathcal{A}^{\dagger}_{1\mu}(pn)\mathcal{A}^{\dagger}_{1,-\mu}(p'n')+\mathcal{A}_{1,-\mu}(p'n')\mathcal{A}_{1\mu}(pn)\right)(-)^{1-\mu}.$$

The equations of motion of the operators defining the phonon operator are determined by the commutation relations:

$$\left[\mathcal{A}_{1\mu}(pn),\mathcal{A}^{\dagger}_{1\mu'}(p'n')\right]\approx\delta_{\mu,\mu'}\delta_{j_p,j_{p'}}\delta_{j_n,j_{n'}}\times$$
$$\left[U_p^2-U_n^2+\frac{U_n^2-V_n^2}{\hat{I}_n^2}\hat{N}_n-\frac{U_p^2-V_p^2}{\hat{I}_p^2}\hat{N}_p\right]. \quad (18)$$

The quasi-boson approximation replaces the r.h. side of the above equation by its average with the $GRFRpnQRPA$ vacuum state, denoted by:

$$D_1(pn)=U_p^2-U_n^2+\frac{1}{2I_n+1}(U_n^2-V_n^2)\langle\hat{N}_n\rangle-\frac{1}{2I_p+1}(U_p^2-V_p^2)\langle\hat{N}_p\rangle. \quad (19)$$

The equations of motion show that the two *qp* energies are also renormalized:

$$E^{ren}(pn)=E_p(U_p^2-V_p^2)+E_n(V_n^2-U_n^2). \quad (20)$$

Here an important difference with respect to the FRpnQRPA equations should be pointed out. There, the quasiparticle energies defining the poles in the dispersion equation for the $FRpnQRPA$ roots are of the types E_p+E_n and E_p-E_n. They show up due to the commutation relations of the basic operators involved in the phonon operator with the independent quasiparticle term of the model Hamiltonian. The difference is caused by the gauge projection operation. The space of pn dipole states, $\mathcal{S}$, is written as a sum of three subspaces defined as:

$$\begin{aligned}
&\mathcal{S}_{+}=\{(p,n)|D_1(pn)>0,\ E^{ren}(pn)>0,\},\\
&\mathcal{S}_{-}=\{(p,n)|D_1(pn)<0,\ E^{ren}(pn)<0,\},\\
&\mathcal{S}_{sp}=\mathcal{S}-(\mathcal{S}_{+}+\mathcal{S}_{-}),\\
&\mathcal{N}_{\pm}=\dim(\mathcal{S}_{\pm}),\ \mathcal{N}_{sp}=\dim(\mathcal{S}_{sp}),\\
&\mathcal{N}=\mathcal{N}_{+}+\mathcal{N}_{-}+\mathcal{N}_{sp}.
\end{aligned} \tag{21}$$

The third line of the above equations specifies the dimensions of these subspaces. In $\mathcal{S}_{+}$ one defines the renormalized operators:

$$\bar{\mathcal{A}}^{\dagger}_{1\mu}(pn)=\frac{1}{\sqrt{D_1(pn)}}\mathcal{A}^{\dagger}_{1\mu}(pn),\quad \bar{\mathcal{A}}_{1\mu}(pn)=\frac{1}{\sqrt{D_1(pn)}}\mathcal{A}_{1\mu}(pn), \tag{22}$$

while in $\mathcal{S}_{-}$ the renormalized operators are:

$$\bar{\mathcal{F}}^{\dagger}_{1\mu}(pn)=\frac{1}{\sqrt{|D_1(pn)|}}\mathcal{A}_{1\mu}(pn),\quad \bar{\mathcal{F}}_{1\mu}(pn)=\frac{1}{\sqrt{|D_1(pn)|}}\mathcal{A}^{\dagger}_{1\mu}(pn). \tag{23}$$

Indeed, the operator pairs $\mathcal{A}_{1\mu},\mathcal{A}^{\dagger}_{1\mu}$ and $\mathcal{F}_{1\mu},\mathcal{F}^{\dagger}_{1\mu}$ satisfy commutation relations of boson type. An $pnQRPA$ treatment within $\mathcal{S}_{sp}$ would yield either vanishing or negative energies. The corresponding states are therefore spurious. $FRpnQRPA$ with the gauge symmetry projected defines the phonon operator as:

$$\Gamma^{\dagger}_{1\mu}=\sum_k\left[X(k)\bar{\mathcal{A}}^{\dagger}_{1\mu}(k)+Z(k)\bar{\mathcal{F}}^{\dagger}_{1\mu}(k)-Y(k)\bar{\mathcal{A}}_{1-\mu}(k)(-)^{1-\mu}-W(k)\bar{\mathcal{F}}_{1-\mu}(k)(-)^{1-\mu}\right], \tag{24}$$

The summation in the defining equation (24) is restricted to the the existence domain of the operators to which is applied. Thus, when the term is containing one of the operators $\bar{\mathcal{A}}^{\dagger}_{1\mu}(k),\bar{\mathcal{A}}_{1-\mu}(k)(-)^{1-\mu}$, then $k\in\mathcal{S}_{+}$. Also, for the terms involving the operators $\bar{\mathcal{F}}_{1\mu},\bar{\mathcal{F}}^{\dagger}_{1\mu}$ the summation is restricted to $k\in\mathcal{S}_{-}$.

The phonon amplitudes are determined by the equations:

$$\left[H,\Gamma^{\dagger}_{1\mu}\right]=\omega\Gamma^{\dagger}_{1\mu},\ \left[\Gamma_{1\mu},\Gamma^{\dagger}_{1\mu'}\right]=\delta_{\mu,\mu'}. \tag{25}$$

Thus, the phonon amplitudes are obtained by solving the $GRFRpnQRPA$ equations:

$$\begin{pmatrix}A_{11}&A_{12}&B_{11}&B_{12}\\A_{21}&A_{22}&B_{21}&B_{22}\\B_{11}&-B_{12}&-A_{11}&-A_{12}\\-B_{21}&-B_{22}&-A_{21}&-A_{22}\end{pmatrix}\begin{pmatrix}X(pn)\\Z(pn)\\Y(pn)\\W(pn)\end{pmatrix}=\omega\begin{pmatrix}X(p_1n_1)\\Z(p_1n_1)\\Y(p_1n_1)\\W(p_1n_1)\end{pmatrix}, \tag{26}$$

where the involved matrices are analytically given in Appendix A.

Matrix dimension for A_{11} and B_{11} is $\mathcal{N}_{+}\times\mathcal{N}_{+}$, while for A_{22} and B_{22} is $\mathcal{N}_{-}\times\mathcal{N}_{-}$. The off diagonal sub-matrices A_{12} and B_{12} have the dimension $\mathcal{N}_{+}\times\mathcal{N}_{-}$, while A_{12} and B_{12} are of the $\mathcal{N}_{-}\times\mathcal{N}_{+}$ type.

In order to solve Eqs.(26) we need to know $D_1(pn)$ and, therefore, the averages of the qp's number operators, $\hat{N}_p$ and $\hat{N}_n$. These are written first in particle representation and then the particle number conserving term is expressed as a linear combination of $\mathcal{A}^\dagger\mathcal{A}$ and $\mathcal{F}^\dagger\mathcal{F}$ chosen such that their commutators with $\mathcal{A}^\dagger, \mathcal{A}$ and $\mathcal{F}^\dagger, \mathcal{F}$ are preserved. The final result is:

$$
\begin{aligned}
\langle \hat{N}_p \rangle &= V_p^2(2I_p+1) + 3(U_p^2 - V_p^2) \\
&\left(\sum_{\substack{n',k \\ (p,n')\in\mathcal{S}_+}} D_1(p,n') \left[Y_k(p,n')\right]^2 - \sum_{\substack{n',k \\ (p,n')\in\mathcal{S}_-}} D_1(p,n^{'}) \left[W_k(p,n')\right]^2 \right), \\
\langle \hat{N}_n \rangle &= V_n^2(2I_n+1) + 3(U_n^2 - V_n^2) \\
&\left(\sum_{\substack{p',k \\ (p',n)\in\mathcal{S}_+}} D_1(p',n) \left[Y_k(p',n)\right]^2 - \sum_{\substack{p',k \\ (p',n)\in\mathcal{S}_-}} D_1(p',n) \left[W_k(p',n)\right]^2 \right).
\end{aligned}
\tag{27}
$$

Eqs.(26), (27) and (19) are to be simultaneously considered and solved iteratively. It is worth mentioning that using the quasiparticle representation for the basic operators $\mathcal{A}^\dagger_{1\mu}$, $\mathcal{F}^\dagger_{1\mu}$, $\mathcal{A}_{1,-\mu}(-1)^{1-\mu}$, $\mathcal{F}_{1,-\mu}(-)^{1-\mu}$ – see Eqs.(13), (22) and (23) – one obtains for $\Gamma^\dagger_{1\mu}$ an expression which involves the scattering pn operators. Thus, the present approach is, indeed, the *GRFRpnQRPA*.

4. THE $2\nu\beta\beta$ PROCESS

The formalism presented above was used to describe the $2\nu\beta\beta$ process. If the energy carried by leptons in the intermediate state is approximated by the sum of the rest energy of the emitted electron and half the Q-value of the double beta decay process

$$\Delta E = \frac{1}{2}Q_{\beta\beta} + m_e c^2, \tag{28}$$

the reciprocal value of the $2\nu\beta\beta$ half-life can be factorized as:

$$(T_{1/2}^{2\nu\beta\beta})^{-1} = F|M_{GT}(0_i^+ \to 0_f^+)|^2, \tag{29}$$

where F is an integral on the phase space, independent of the nuclear structure, while M_{GT} stands for the Gamow-Teller transition amplitude and has the expression:

$$M_{GT} = \sqrt{3}\sum_{k,k'} \frac{{}_i\langle 0||\beta_i^+||1_k\rangle_{ii}\langle 1_k|1_{k'}\rangle_{ff}\langle 1_{k'}||\beta_f^+||0\rangle_f}{E_k + \Delta E + E_{1^+}}. \tag{30}$$

In the above equation, the denominator consists of three terms: a) ΔE, which was already defined, b) the average value of the k-th $GRFRpnQRPA$ energies in mother and daughter nuclei respectively, normalized to the particular value corresponding to k=1, and c) the experimental energy for the lowest 1^+ state. The indices carried by the β^+ operators indicate that they act in the space spanned by the $GRFRpnQRPA$ states associated to the initial (i) or final (f) nucleus. The overlap m.e. of the single phonon states in the initial and final nuclei respectively, are calculated within $GRFRpnQRPA$. In Eq.(30), the Rose convention for the reduced m.e. is used [25].

Note that if we restrict the pn space to $\mathcal{S}_+$ and, moreover, the dipole-pairing interaction is ignored, M_{GT} vanishes due to the second leg of the transition. Indeed, the m.e. associated to the daughter nucleus is of the type ${}_f\langle 0|(c_n^\dagger c_p)_{1\mu}(c_n^\dagger c_p)_{1\mu}|o\rangle_f$, which is equal to zero due to the Pauli principle restriction. In this case the equations of motion are of Tamm-Dankoff type and, therefore, the ground state correlations are missing. In order to induce the necessary correlations we have either to extend the formalism in the space $\mathcal{S}_-$, or to allow the ph excitations to interact via a pairing like force. Also, we remark that the operator $\bar{\mathcal{A}}^\dagger_{1\mu}$ plays the role of a β^- transition operator, while when $\bar{\mathcal{F}}^\dagger_{1\mu}$ or $\mathcal{A}_{1\mu}$ is applied on the ground state of the daughter nucleus, a β^+ transition is induced. Therefore, the 2β decay cannot be described by considering the β^- transition alone.

5. NUMERICAL APPLICATION AND DISCUSSIONS

The approach presented in the previous sections was applied for the transitions of fourteen double beta emitters: ^{48}Ca, ^{76}Ge, ^{82}Se, ^{96}Zr, ^{100}Mo, ^{104}Ru, ^{110}Pd, ^{116}Cd, ^{128,130}Te, ^{148,150}Nd, ^{154}Sm, and ^{160}Gd. We present first the parameters involved in our calculations.

5.1. PARAMETERS

The parameters defining the single particle energies are those of the spherical shell model, the deformation parameter d and the parameter k relating the quadrupole coordinate with the quadrupole bosons, as shown in Eq.(3). These are fixed as described in Ref. [19]. The proton and neutron pairing strengths are slightly different from those from the quoted reference since the dimension of the single particle basis used in the present paper is different from that from Ref. [19]. The strength of the dipole pn two-body interaction was taken to be

$$\chi = \frac{5.2}{A^{0.7}} MeV. \tag{31}$$

This expression was obtained by fitting the positions of the GT resonances in ^{40}Ca, ^{90}Zr and ^{208}Pb [26]. The strength for the attractive pn two-body interaction was chosen so that the result for the $\log\ ft$ value associated to one of the single beta decay of the intermediate odd-odd nucleus, be close to the corresponding experimental data. If the experimental data are missing, the restriction refers to the existent data in the neighboring region. Since for ^{100}Mo and ^{116}Cd, experimental data for the $\log\ ft$ values associated to the $\beta^{\pm}$ decays of the intermediate odd-odd nuclei ^{100}Tc and ^{116}In respectively, are available, the parameters χ and χ_1 were fixed such that the mentioned data are reproduced. The results for the fitted parameters are given in Table I. There, we give also the result for the Ikeda Sum Rule (ISR).

The BCS calculations are performed by using a certain number of states outside an inert core. The core system for the fourteen decays is defined by the (Z,N), listed in Table II. Therein, one may find also the number of single particle double degenerate states used in our calculations. In order to perform the $GRFRpnQRPA$ we have to divide the space of proton-neutron dipole states, $\mathcal{S}$, into three subspaces ($\mathcal{S}_+,\mathcal{S}_-,\mathcal{S}_{sp}$), according to the definition given by Eq. (21). The dimensions for the spaces ($\mathcal{S}_+,\mathcal{S}_-,\mathcal{S}$) for the mother ($D_1$) and daughter ($D_2$) nuclei are also listed. As explain in the body of the previous sections, the $GRFRpnQRPA$ equations together with the constraint equations are to be solved iteratively. In Table II, we give the number of iterations which are necessary in order to achieve the process convergence.

5.2. SINGLE BETA TRANSITION STRENGTHS $B(GT^{\pm})$

Since the double beta matrix elements are expressed as a product of two reduced matrix elements, one associated to the β^- transition of the mother nucleus, while the second one to the β^+ transition of the daughter nucleus, it is worthwhile to study the strength distribution over the $GRFRpnQRPA$ energies, for the two transitions. Using the data shown in Tables I and II as input, we calculated the distribution of the $\beta^{\pm}$ strengths with the result shown in Figs.1-4. The energy intervals where both strengths are large, contribute significantly to the double beta transition amplitude. The β^- strength is fragmented among the $GRFRpnQRPA$ states reflecting the fact that the single particle states are deformed. The β^- strengths for the emitters considered in Fig. 1 exhibit three major peaks. ^{48}Ca and ^{76}Ge have one additional small bump, close to the last and intermediate major peaks, respectively. The β^- strength of ^{48}Ca has been studied in Ref. [39] where the GT resonance has been populated in the reaction $^{48}Ca(p,n)^{48}Sc$. It was shown that the GT resonance is spread over an energy interval between 4.5 and 14.5 MeV. As seen from Fig.1, the results of our calculations concerning the width of the GT resonance agree with the mentioned experimental data. In ^{76}Ge and ^{82}Se the strength distribution has been studied in the reactions $^{76}_{32}Ge(p,n)^{76}_{33}As$ and $^{82}_{34}Se(p,n)^{82}_{35}Br$ [41], respectively. The B(GT) values have been extracted from the excitation energy spectrum. These values

Table 1.

The deformation parameter d, the pairing interaction strengths for protons (G_p) and neutrons (G_n), the GT dipole (χ) and dipole-pairing (X_{dp}) interaction strengths used in our calculations. We also give the parameter k relating the quadrupole coordinates and bosons (this is involved in the expression of the single particle energies). Results for $ISR/3$ are to be compared with the corresponding $N-Z$ values.

	d	k	G_p[MeV]	G_n[MeV]	$ISR/3$	$\chi[MeV]$	$X_{dp}[MeV]$
^{48}Ca	0.3	8.	0.42	0.43	8.04	0.346	0.253
^{48}Ti	0.05	8.	0.46	0.36	4.04	0.346	0.253
^{76}Ge	1.6	10.	0.22	0.382	11.99	0.250	0.609
^{76}Se	1.9	10.	0.24	0.325	7.99	0.250	0.609
^{82}Se	0.2	9.	0.261	0.344	14.00	0.238	0.143
^{82}Kr	0.2	9.	0.24	0.268	10.01	0.238	0.143
^{96}Zr	1.5	12.	0.18	0.343	16.08	0.213	0.106
^{96}Mo	1.2	10.	0.22	0.338	11.99	0.213	0.106
^{100}Mo	-1.5	5.5	0.18	0.288	15.995	0.232	1.406
^{100}Ru	-0.6	5.5	0.15	0.255	12.002	0.232	1.406
^{104}Ru	-1.55	12.	0.18	0.35	16.00	0.201	0.502
^{104}Pd	-1.35	9.	0.18	0.275	12.00	0.201	0.502
^{110}Pd	-1.6	10.	0.16	0.306	18.05	0.194	0.775
^{110}Cd	-0.8	10.	0.16	0.3105	13.97	0.194	0.775
^{116}Cd	-1.8	12.	0.15	0.282	20.07	0.2	1.308
^{116}Sn	-1.2	12.	0.12	0.2458	16.007	0.2	1.308
^{128}Te	0.5	8.	0.12	0.266	24.05	0.450	0.436
^{128}Xe	1.7	8.	0.12	0.2518	20.02	0.450	0.436
^{130}Te	0.493	12.	0.10	0.292	26.00	0.7	0.840
^{130}Xe	1.4	12.	0.11	0.286	21.94	0.7	0.840
^{148}Nd	1.555	14.	0.11	0.2516	28.02	0.157	0.142
^{148}Sm	0.1555	14.	0.11	0.225	24.04	0.157	0.142
^{150}Nd	1.952	16.	0.10	0.254	30.05	0.156	0.016
^{150}Sm	1.952	16.	0.11	0.235	26.08	0.156	0.016
^{154}Sm	2.29	16.	0.10	0.316	30.08	0.153	0.138
^{154}Gd	2.29	14.	0.11	0.27	26.01	0.153	0.138
^{160}Gd	2.714	10.	0.11	0.3	32.07	0.149	0.298
^{160}Dy	2.714	8.	0.11	0.2578	28.02	0.149	0.298

Table 2.

The number of single particle proton states lying above the (Z,N) core is given. The single particle space for neutrons is identical to that for protons. D_1 and D_2 are the dimensions of the spaces $\mathcal{S}_+, \mathcal{S}_-, \mathcal{S}$ defined in the text, for the mother and daughter nuclei, respectively. The dimension of the $GRFRpnQRPA$ matrix is equal to the sum of the $\mathcal{S}_+$ and $\mathcal{S}_-$ dimensions. Also, the number of steps necessary for the iterative procedure convergence, are listed.

Nucleus	core's (Z,N)	Number of states	D_1	D_2	Number of iterations
^{48}Ca	(0,0)	31	(96,0,103)	(79,7,103)	7
^{76}Ge	(20,20)	31	(96,0,119)	(83,0,119)	5
^{82}Se	(20,20)	37	(107,0,135)	(95,0,135)	4
^{96}Zr	(20,20)	39	(116,0,141)	(105,8,141)	15
^{100}Mo	(20,20)	46	(137,1,163)	(139,2, 175)	8
^{104}Ru	(26,26)	39	(118,1,140)	(111,2,140)	7
^{110}Pd	(26,26)	43	(146,0,162)	(125,7,162)	6
^{116}Cd	(20,20)	55	(189,0,219)	(182,4,219)	8
^{128}Te	(28,28)	60	(191,0,228)	(185,1,232)	5
^{130}Te	(42,42)	67	(204,0,242)	(182,0,244)	6
^{148}Nd	(40,40)	51	(158,3,203)	(168,1,203)	5
^{150}Nd	(40,40)	57	(203,2,246)	(197,1,246)	4
^{154}Sm	(40,40)	57	(203,0,249)	(204,3,249)	9
^{160}Gd	(40,40)	59	(216,1,253)	(215,0,253)	14

have been folded with a Gaussian with a width of 1 MeV and plotted in Fig. 1 to be compared with the results of our calculation. We notice that the centroids of the large peaks from ^{76}Ge lie close to those shown by the experimental data. Concerning ^{82}Se, the large peak is nicely described. The centroids of the two smaller peaks lie close to the peaks predicted by our calculations. It is worth mentioning that it is hard to make a fair comparison between the magnitudes of the peaks in our calculations and those extracted from the experimental data. Indeed, the total experimental $B'(GT^-)$ strengths for ^{76}Ge and ^{82}Se represent only 65 and 59% respectively, from the (N-Z) value [41]. We notice that the β^- strength has a little bump below 2.5 MeV which is specific to the fully renormalized formalism, this strength being carried by the scattering terms amplitude. The new terms in the phonon operator manifest even more clearly in the β^+ strength where in three cases a peak close to zero shows up. Note that while in the β^- case there is no strength beyond the last major peak, for the β^+ case small peaks show up after the major peak. This feature is most evident in ^{76}Se and ^{82}Kr. Due to the overlap of their energy spread with that of the major peak in the distribution of the β^- strength, they contribute significantly to the GT transition amplitude.

The distribution of the $\beta^\pm$ strengths for ^{100}Mo and ^{116}Cd is shown in Fig.2. Again, the $\beta^\mp$ strengths are fragmented among the $pnQRPA$ states, reflecting the fact that the single particle states are deformed. Note that the first peak for the β^- strength is the highest one, while the one centered at higher energy has a large width and a fine substructure. The low energy peak is mainly determined by the attractive two-body interaction while the broad peak, *i.e.* the GT giant resonance, by the ph interaction. The β^+ strength is small in magnitude and less fragmented than the β^- strength. Also we note that the highest energy peak is the largest one.

The β^- strengths shown in Fig. 3 exhibit some specific features. ^{104}Ru and ^{110}Pd have a low energy peak centered at about 1 MeV, while the GTR is spread over a wide interval ranging from 2.5 to 12.8 MeV with the strength shared mainly by three peaks. The β^- strength distributions for ^{128}Te and ^{130}Te start with a wide peak spread over the interval 0 to 5 MeV and continue with the GTR located between 5 and 14 MeV. The experimental β^- strength for these nuclei were extracted from the excitation energy spectrum at 0.3 deg and 134.4 MeV, measured in the reactions ^{128}Te(p,n)^{128}I and ^{130}Te(p,n)^{130}I, respectively [41]. Our calculations confirm the three peak and four peak structure in the two nuclei. However, the highest peak in our calculations is the first one while the experimental dominant peak is the last one, located at 13.14 MEV in ^{128}Te and 13.59 MeV in ^{130}Te [41]. Also, we note that the theoretical peaks are not sharply separated as suggested by the experimental data after eliminating the background contribution to the GTR.

Again, the relevance of comparing the results with the corresponding experimental data is dictated by the fact that the total experimental $B'(GT^-)$ strengths for ^{128}Te and ^{130}Te, accounting also for the contribution of the background, represent only 72 and 71$\%$ respectively, from the (N-Z) value [41]. Eliminating the background contribution to the total strength, as happens in Fig. 3, the total measured strength amounts about 56 and 59$\%$, respectively. The β^- strength seen below 2.5MeV, which is specific to the fully renormalized formalism, seems to be carried by the scattering terms amplitude. The new terms in the phonon operator manifest also in the β^+ strength distribution where in three cases a peak close to zero shows up. While for the first two nuclei the dominant peaks in the β^+ strength are in the low energy region for the two isotopes of Te the peak centroid energies are almost identical to the corresponding GTR centroid energies.

The β^- strength distributions for the double beta emitters ^{148,150}Nd, ^{154}Sm and ^{160}Gd are presented in Fig. 4. For the first two transitions the β^- strength has a dominant peak, which is just the GT resonance. For ^{154}Sm and ^{160}Gd, one and two additional peaks show up at lower energy and with a height comparable to that of the GT resonance. The β^+ strength is also fragmented but exhibits a single dominant peak located at an energy close to the GT resonance centroid. For the transitions of ^{154}Gd and ^{160}Dy an important amount of strength is accumulated in the low part of the spectrum. Actually this appear to be an effect caused by the scattering terms from the phonon operator.

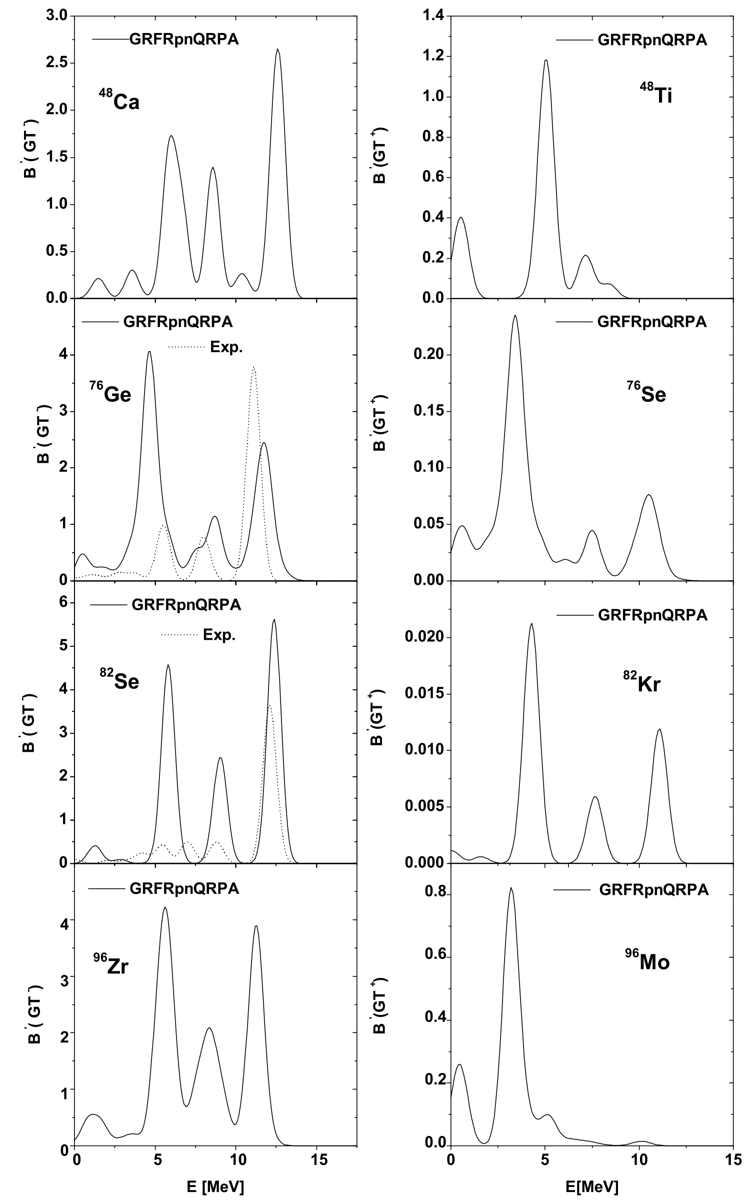

Fig. 1 – One third of the single β^- (left column) and one third of the β^+ (right column) strengths, denoted by $B'(GT^-)$ and $B'(GT^+)$, for the mother , ^{48}Ca, ^{76}Ge, ^{82}Se and ^{96}Zr, and daughter, ^{48}Ti, ^{76}De, ^{82}Kr and ^{96}Mo, nuclei respectively, folded by a Gaussian function with a width of 1 MeV, are plotted as functions of the corresponding energies yielded by the present formalism. Note that the difference of the two strengths for the mother nucleus should amount N-Z if the sum rule is obeyed. For ^{76}Ge and ^{82}Se, the experimental data for the β^- strength are also presented.

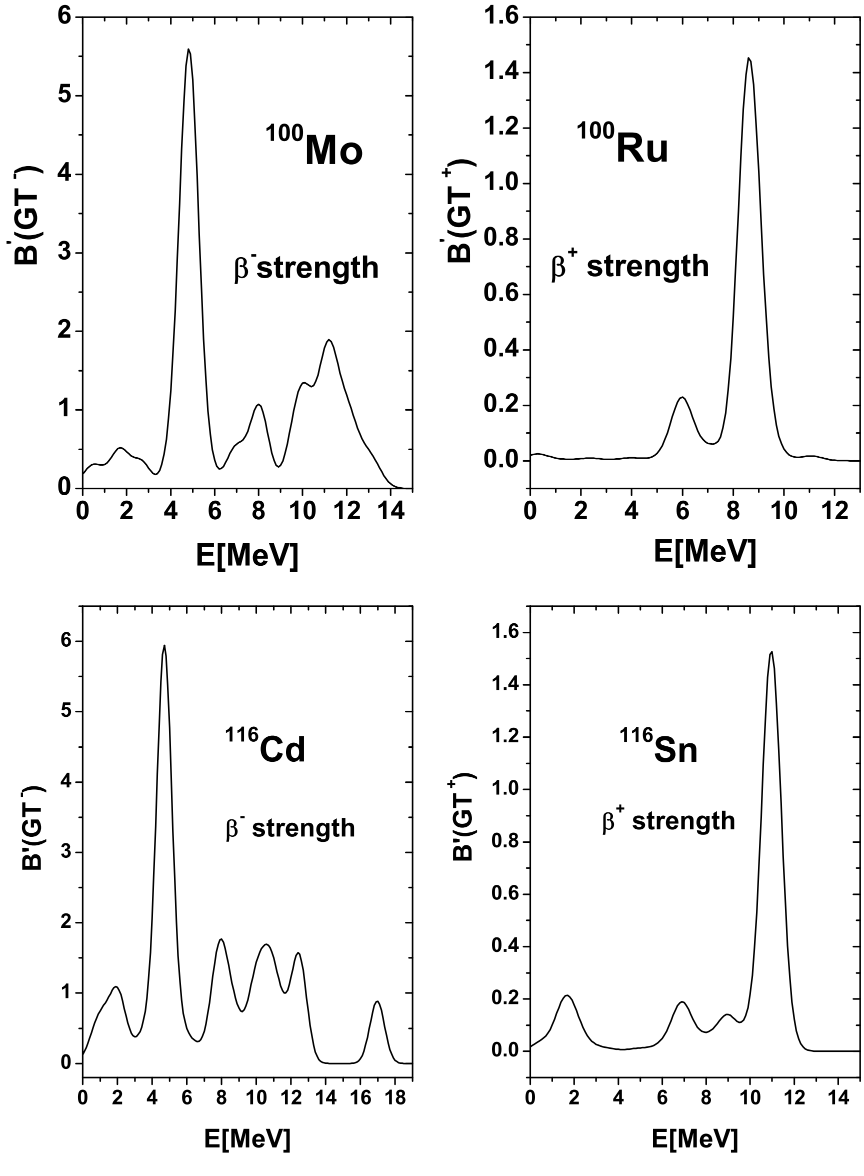

Fig. 2 – The same as in Fig.1 but for the mother nuclei ^{100}Mo (upper-left panel) and ^{116}Cd (bottom-left panel), and the daughter nuclei, ^{100}Ru (upper-right panel) and ^{116}Sn (bottom-right panel).

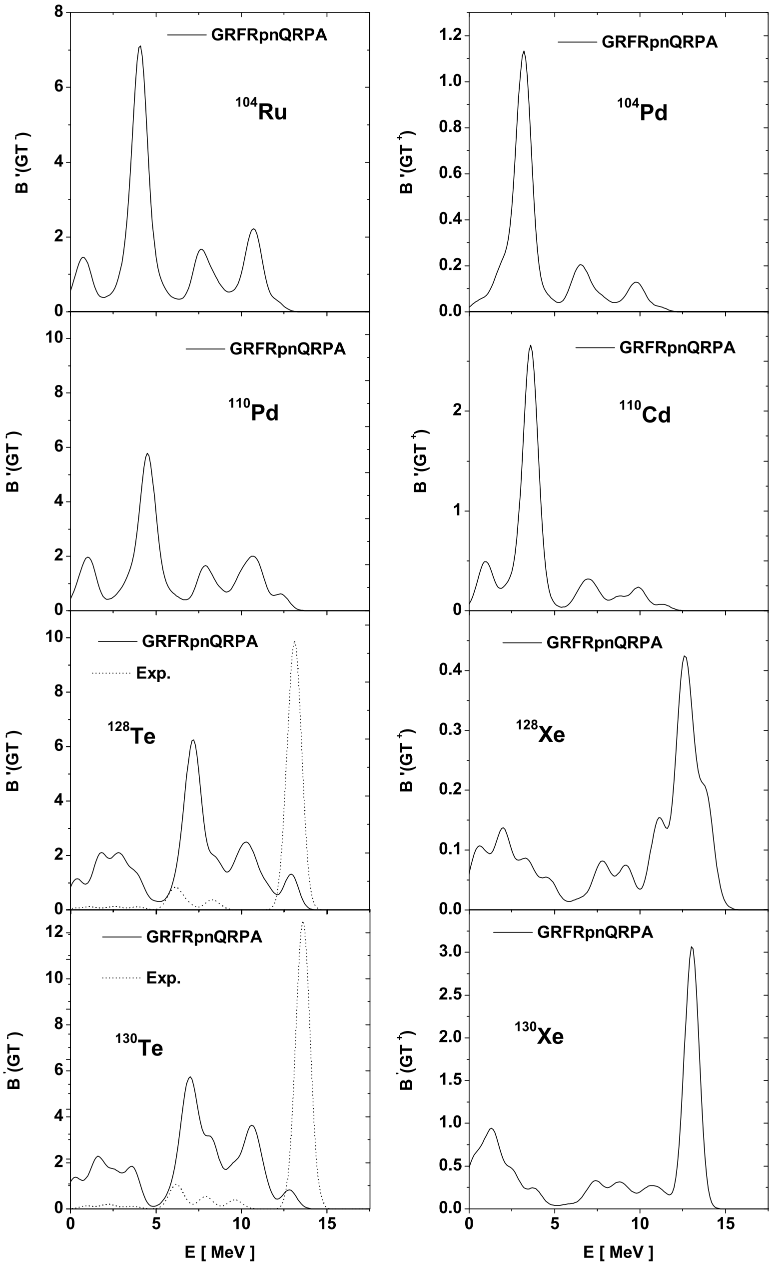

Fig. 3 – The same as in Fig. 1 but for the mother nuclei ^{104}Ru, ^{110}Pd, ^{128,130}Te and the daughter nuclei ^{104}Pd, ^{110}Cd, ^{128,130}Xe, respectively. For ^{128,130}Te, the experimental data are also presented.

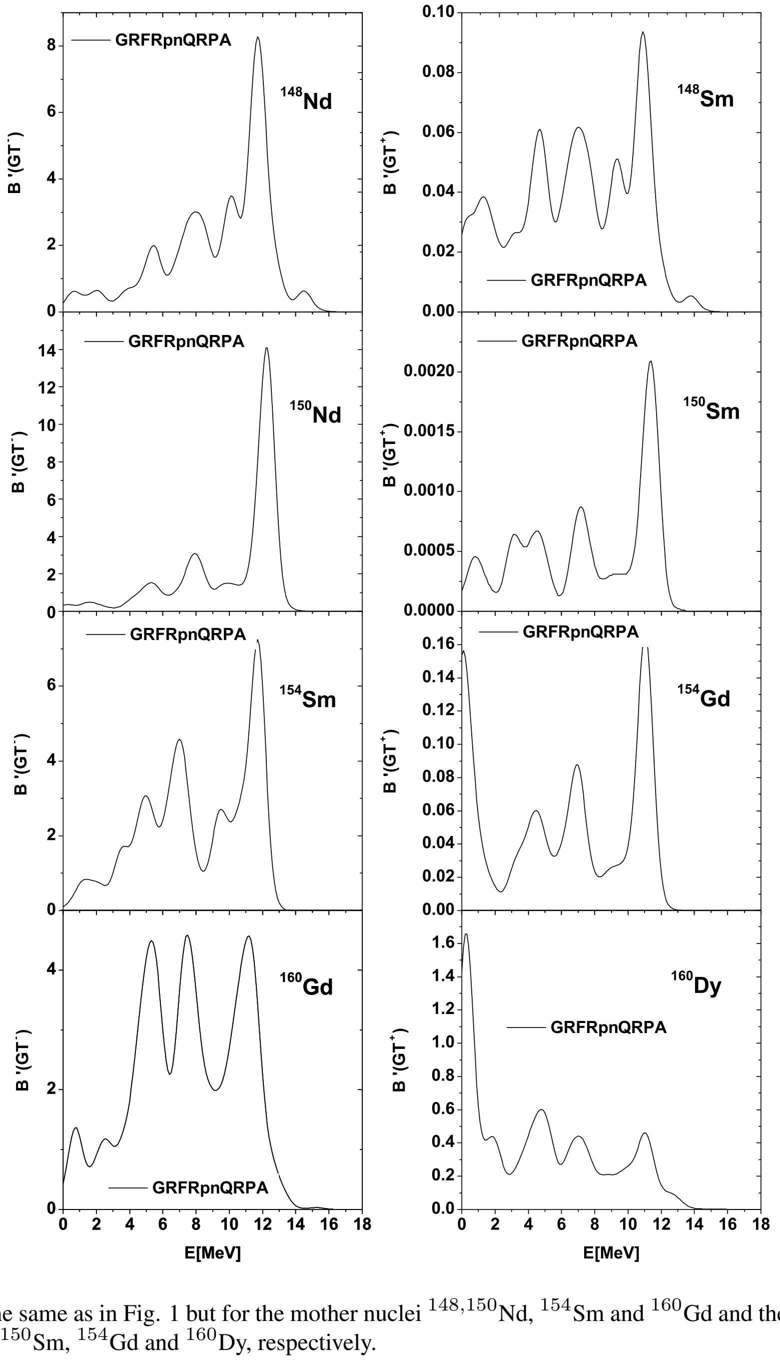

Fig. 4 – The same as in Fig. 1 but for the mother nuclei ^{148,150}Nd, ^{154}Sm and ^{160}Gd and the daughter nuclei ^{148,150}Sm, ^{154}Gd and ^{160}Dy, respectively.

Table 3.

The calculated summed strengths for the β^- strength associated to the mother nuclei and the summed β^+ strengths for the daughter nuclei, quenched by a factor 0.6, are compared with the corresponding available data. Experimental data for total B(GT$^-$) are taken from Refs. [38] ($^{a)}$), [41] ($^{b)}$), [42] ($^{c)}$), [45] ($^{d)}$), [47] ($^{e)}$, $^{f)}$

Nucleus	$0.6\sum B(GT)^-$	$\sum\left[B(GT)^-\right]_{exp}$	Nucleus	$0.6\sum B(GT)^+$	$\sum\left[B(GT)^+\right]_{exp}$
^{48}Ca	14.54	14.4±2.5 $^{a)}$	^{48}Ti	3.666	1.9±0.5 $^{a)}$
^{76}Ge	23.037	23.3 $^{b)}$	^{76}Se	1.125	1.45±0.07 $^{c)}$
^{82}Se	25.372	24.6 $^{b)}$	^{82}Kr	0.079	-
^{96}Zr	29.163	-	^{96}Mo	2.537	0.29±0.08 $^{d)}$
^{100}Mo	28.96	26.69 $^{e)}$	^{100}Ru	-	-
^{104}Ru	32.921	-	^{104}Pd	3.990	-
^{110}Pd	32.932	-	^{110}Cd	7.239	-
^{116}Cd	36.2	32.7 $^{f)}$	^{116}Sn	-	-
^{128}Te	43.485	40.08 $^{b)}$	^{128}Xe	2.917	-
^{130}Te	47.432	45.90 $^{b)}$	^{130}Xe	13.040	-
^{148}Nd	51.74	-	^{148}Sm	1.29	-
^{150}Nd	54.11	-	^{150}Sm	0.02	-
^{154}Sm	54.68	-	^{154}Gd	0.54	-
^{160}Gd	57.93	-	^{160}Dy	0.21	-

.

As seen from Table I the results of our calculations for single beta transition strengths obey the ISR.

An interesting result which is worth to be mentioned, concerns the summed strength for the β^- and β^+ transition, denoted conventionally, by $\sum B(GT^-)$ and $\sum B(GT^+)$, respectively. These single β decay strengths quenched with a factor of 0.6 [37], accounting for the polarization effects on the single-β transition operator, ignored in the present paper, are listed in Table III. Actually, the quenched values are to be compared with the experimental data, since the measured B(GT) strength represents about 60%-70% of the strength corresponding to the ISR.

The experimental value for the summed $B(GT^-)$ of ^{48}Ca is taken from Ref. [38], where from the total strength, which amounts about 15.3±2.2, the contribution of isovector spin monopole states was extracted. The result was obtained with the reaction ^{48}Ca(p,n)^{48}Sc, and corresponds to a large energy excitation interval, from 0 to 30 MeV.

In [41] the total GT strength, for ^{76}Ge and ^{82}Se, consists of the sum of the strength observed in the peaks plus the estimated contribution from the background. The experimental results correspond to 65 and 59% of the 3(N-Z) sum rule. According to Ref. [39], by adding to the GT cross section in discrete states the contribution from the background and that of continuum, the total strength magnitude is much improved to a better obey of the sum rule. We note a good agreement between the results of our calculations for the summed β^- strength and the corresponding experimental data.

The experimental data for the summed $B(GT^+)$ transition of ^{48}Ti was taken from [38]. This result was obtained after extracting the contribution of the isovector spin monopole states from the total strength of 2.8±0.3. The reaction ^{48}Ti(n,p)^{48}Sc was used to study the $B(GT^+)$ strength for excitation energies up to 30 MeV. This value for the total strength is larger than that reported by Alford *et al.* [40]

$$\sum B(GT^+) = 1.42 \pm 0.2. \tag{32}$$

where only contribution of states with excitation energies up to 15 MeV are taken into account. This comparison shows that, indeed, the B(GT) strength is sensitive to the magnitude of the considered energy interval. In this context we mention the results obtained through the charge exchange reactions (^{3}He,t) and (d,^{2}He) on ^{48}Ca and ^{48}Ni respectively [43], for $B(GT^-)$ and $B(GT^+)$ with an excitation energy interval $E_x \leq 5$ MeV: 1.43(38), 0.45.

The GT strength from the ^{76}Se(n,p)^{76}As reaction [42] is 1.45 ± 0.07 and corresponds to and excitation energy $E_x \leq 10MeV$. The authors used the multipole decomposition method. In Ref. [44] the $B(GT^+)$ strength was measured in a different reaction, ^{76}Se(d,^{2}He)^{76}As, and different excitation energy interval, $E_x \leq 4MeV$. The result reported is $\sum_{0-4MeV} B(GT^+) = 0.54 \pm 0.1$, which is smaller than that from Ref. [42]. The length of the energy intervals justifies the mentioned differences. We remark that the results for the summed β^+ strength in ^{48}Ti and ^{76}Se are in reasonable good agreement with the corresponding experimental data.

The last β^+ strength mentioned in Table 3 refers to the daughter nucleus ^{96}Mo. Through the reaction ^{96}Mo(d,^{2}He)^{96}Nb the strength taken mainly by a single state, placed at 0.69 MeV, was measured. However, from Fig.1 we note that, indeed, there is a state at 0.69 Mev which catch a certain β^+ strength, but that strength is smaller than that distributed among the states lying in the energy interval of 1.8 to 7.5 MeV. More complete measurement through a (p,n) reaction on ^{96}Mo and an energy range of 0-10 MeV is necessary in order to make a fair comparison with the results presented here. The matrix elements involved in the double beta transition amplitude of ^{100}Mo and ^{116}Cd, have been experimentally investigated in Ref. [47]. The first matrix elements, describing the transitions $0^+_i \rightarrow 1^+$, were obtained from the reactions ^{100}Mo(^{3}He,t)^{100}Tc and ^{116}Cd(^{3}He,t)^{116}In respectively, at $\theta_t \approx 0^0$, while the matrix elements for the $1^+ \rightarrow 0^+_f$ were derived from the known $\log\ ft$ value. For both cases the strength of the first β^- transition exhibits two bumps, one broad and called GTR1 while the second one less spread, located at lower energy and called GTR2. The centroid energies of the two resonances as well as the strength carried by each of them are compared with the theoretical results obtained with our approach, in Table 4. The quenched values of the total β^- strength of ^{128,130}Te are compared with the experimental data since the measured $B(GT^-)$ strength, as we already mentioned before, represents about 56% and 59% respectively, of the strength corresponding to the ISR. There are some claims [39] saying that adding the strength carried by the states from the continuum, the total B(GT) strength are corrected up to 90% of the simple sum rule. We remark the good agreement between the calculated and experimental total strength. Note that if we replace the quenching factor by 0.56 for ^{128}Te and by 0.59 for ^{130}Te the results for the total strength would be 40.586 and 46.56 respectively which are closer to the experimental data. Unfortunately for the last four mother and for the last four daughter nuclei, there are no data available for the single β^- and single β^+ strengths, respectively.

5.3. TRANSITION AMPLITUDE AND HALF LIFE

The energy corrections involved in Eq.(30) for the considered double beta emitters, are:

$$\begin{array}{ll}
\Delta E(^{48}\mathrm{Ca}) = 2.646 \text{ MeV}, & E_{1^+}(^{48}\mathrm{Sc})=0.338 \text{ MeV}, \\
\Delta E(^{76}\mathrm{Ge}) = 1.530 \text{ MeV}, & E_{1^+}(^{76}\mathrm{As})=0.044 \text{ MeV}, \\
\Delta E(^{82}\mathrm{Se}) = 2.016 \text{ MeV}, & E_{1^+}(^{82}\mathrm{Br})=0.075 \text{ MeV}, \\
\Delta E(^{96}\mathrm{Zr}) = 2.186 \text{ MeV}, & E_{1^+}(^{160}\mathrm{Nb})=1.116 \text{ MeV}, \\
\Delta E(^{100}\mathrm{Mo}) = 2.026 \text{ MeV}, & E_{1^+}(^{100}\mathrm{Tc})=0.0 \text{ MeV}. \\
\Delta E(^{104}\mathrm{Ru}) = 1.161 \text{ MeV}, & E_{1^+}(^{104}\mathrm{Rh})=0.0 \text{ MeV}, \\
\Delta E(^{104}\mathrm{Pd}) = 1.516 \text{ MeV}, & E_{1^+}(^{110}\mathrm{Ag})=0.0 \text{ MeV}, \\
\Delta E(^{116}\mathrm{Cd}) = 1.916 \text{ MeV}, & E_{1^+}(^{116}\mathrm{In})=0.0 \text{ MeV}, \\
\Delta E(^{128}\mathrm{Te}) = 0.946 \text{ MeV}, & E_{1^+}(^{128}\mathrm{I})=0.58 \text{ MeV}, \\
\Delta E(^{130}\mathrm{Te}) = 1.776 \text{ MeV}, & E_{1^+}(^{130}\mathrm{I})=0.85 \text{ MeV}, \\
\Delta E(^{148}\mathrm{Nd}) = 1.476 \text{ MeV}, & E_{1^+}(^{148}\mathrm{Pm})=0.137 \text{ MeV}, \\
\Delta E(^{150}\mathrm{Nd}) = 2.196 \text{ MeV}, & E_{1^+}(^{150}\mathrm{Pm})=0.137 \text{ MeV}, \\
\Delta E(^{154}\mathrm{Sm}) = 1.530 \text{ MeV}, & E_{1^+}(^{154}\mathrm{Eu})=0.046 \text{ MeV}, \\
\Delta E(^{160}\mathrm{Gd}) = 0.046 \text{ MeV}, & E_{1^+}(^{160}\mathrm{Tb})=0.139 \text{ MeV}.
\end{array} \tag{33}$$

Calculating first the GT transition amplitude and then the Fermi integral with $G_A = 1.254$, as in Ref. [4], we obtained the half-lives given in Table 5. There we also give the experimental data taken from different sources as well as the results obtained by other procedures. From there one can see that the results of our calculations agree quite well with the corresponding experimental data. Results of Ref.[10] were obtained within a standard renormalized $pnQRPA$ formalism and therefore the ISR is violated.

5.4. TRANSITIONS OF THE INTERMEDIATE ODD-ODD NUCLEUS

The intermediate odd-odd nuclei involved in the double beta process can, in principle, perform the transition β^+/EC, which results in feeding the mother nu-

Table 4.

The strengths B(GT) of the single β^- transitions from the mother nuclei to the intermediate odd-odd nuclei excited in the states of the two components, GTR1 and GTR2, of the GT giant resonance are listed. The experimental data taken from Ref. [47](Exp.) and theoretical (Th.) values for the centroid energies of the two resonances are also specified.

Excited states	^{100}Tc				^{116}In			
	Ex[MeV]		B(GT)		Ex[MeV]		B(GT)	
	Exp.	Th.	Exp.	Th.	Exp.	Th	Exp.	Th.
GTR1	13.3	11.16	23.1± 3.8	15.63	14.5	12.37	25.8± 4.1	18.9
GTR2	8.0	8.05	2.9±0.5	5.87	8.9	7.87	6.6±1.1	7.2

cleus of each transition. On the other hand, they can perform a β^- transition to the corresponding daughter nuclei. For some transitions of this type the $\log ft$ values are measured. The corresponding theoretical results are obtained by means of the expression:

$$ft_{\mp} = \frac{6160}{[{}_l\langle 1_1||\beta^{\pm}||0\rangle_l g_A]^2},\; l = i,f. \tag{34}$$

In order to take account of the effect of distant states responsible for the "missing strength" in the giant GT resonance [4] we chose $g_A = 1.0$. In a previous publication [19], where a standard $pnQRPA$ approach was used, the strengths of the ph and pp interactions have been fixed in order to reproduce the $\log\ ft$ values characterizing the two transitions of the intermediate odd-odd nucleus. Similarly, here the strengths of the two body proton-neutron interactions, χ and X_{dp}, could be fixed by fitting the $\log\ ft$ values associated to the two single beta transitions. This procedure has been applied, however, only for ^{100}Mo and ^{116}Cd. Unfortunately, there are not enough available data to enable a fitting procedure for the remaining emitters. For these nuclei the strength of the ph interaction was taken as given by Eq. (31) while the attractive interaction strength was chosen such that one of the decay branches of the odd-odd nuclei has the $\log ft$ value close to those known for the chosen nucleus or for a nucleus from the neighboring region. In Table 6, the results of our calculations for the mentioned $\log\ ft$ values are listed. As seen from Fig.1 the predicted centroid of the GT resonance has a small shift with respect to the experimental one. This suggests that Eq.(31) should be revisited and the fit of the GT resonance centroids be performed within the $GRFRpnQRPA$.

5.5. PREVIOUS CONSIDERATION OF THE SUBJECT

After our paper on fully renormalized $pnQRPA$ was published [11], another approach addressing the same issue showed up [48,49], which claims that the results obey the ISR. However as pointed out in Ref. [50], that formalism does not fulfill the consistency condition, required by the linearizing procedure. Actually, this feature

Table 5.

The Gamow-Teller amplitude for the $2\nu\beta\beta$ decay, in units of MeV^{-1}, and the corresponding half life ($T_{1/2}$), in units of yr, are listed for fourteen ground to ground transitions. The experimental half-life for the transitions were taken from the specified references. Also, comparison is made with the theoretical results from the last three columns, reported in Refs. [18, 19], [34–36] and [10, 63], respectively.

	M_{GT}[MeV^{-1}]	$T_{1/2}$[yr]				
		present	Exp.	Raduta $et al.$ [18, 19]	Klapdor $et\ al.$ [34–36]	Others [10], [63]
^{48}Ca→^{48}Ti	0.045	4.72×10^{19}	$(4.2\pm1.2)\times10^{19}$ [27] $4.4^{+0.6}_{-0.5}\times10^{19}$ [46]	7.48×10^{19}	3.2×10^{19}	-
^{76}Ge→^{76}Se	0.177	0.938×10^{21}	$9.2^{+0.7}_{-0.4}\times10^{20}$ [28] $(1.5\pm0.1)\times10^{21}$ [46]	4.05×10^{20}	2.61×10^{20}	1.4×10^{21} [10]
^{82}Se→^{82}Kr	0.083	1.293×10^{20}	$1.1^{+0.8}_{-0.3}\times10^{20}$ [29] $(0.92\pm0.07)\times10^{20}$ [46]	0.963×10^{20}	0.848×10^{20}	1.1×10^{20} [10]
^{96}Zr→^{96}Mo	0.115	1.59×10^{19}	$(1.4^{+3.5}_{-0.5})\times10^{19}$ [30] $(2.3\pm0.2)\times10^{19}$ [46]	0.44×10^{19}	5.2×10^{17}	4.4×10^{19} [10]
^{100}Mo→^{100}Ru	0.221	$8.79\cdot10^{18}$	$(8.0\pm0.16)\cdot10^{18}$ [30] $(0.115^{+0.03}_{-0.02})\cdot10^{20}$ [31] $0.033^{+0.02}_{-0.01}\cdot10^{20}$ [32, 33]	$4.4\cdot10^{18}$	$2.9\cdot10^{18}$ [59]	$1.8\cdot10^{18}$ [56]
^{104}Ru→^{104}Pd	0.453	2.26×10^{21}	-	0.76×10^{21}	1.8×10^{21} 3.1×10^{22}	-
^{110}Pd→^{110}Cd	0.188	3.11×10^{20}	-	1.58×10^{20}	5.0×10^{19} 1.2×10^{21}	-
^{116}Cd→^{116}Sn	0.15998	$2.02\cdot10^{19}$	$(3.2\pm0.3)\cdot10^{19}$ [47]	$3.86\cdot10^{19}$	$5.1\cdot10^{19}$ [57]	$8.3\cdot10^{18}$ $3.75\cdot10^{19}$ [60]
^{128}Te→^{128}Xe	0.056	1.43×10^{24}	$(7.2\pm0.3)\times10^{24}$ [30] $(1.5\pm0.2)\times10^{24}$ [54] $(1.9\pm0.4)\times10^{24}$ [46]	0.55×10^{24}	1.2×10^{23} 5.7×10^{23}	5.6×10^{23} [10] -
^{130}Te→^{130}Xe	0.023	1.56×10^{21}	$(1.5\text{-}2.8)\times10^{21}$ [30] $(2.7\pm0.1)\times10^{21}$ [54] $(0.7\pm0.3)\times10^{21}$ [55] $(6.8^{+1.2}_{-1.1})\times10^{20}$ [46]	0.26×10^{21}	1.9×10^{19} 1.2×10^{20}	0.26×10^{21} [10] -
^{148}Nd→^{148}Sm	0.422	2.00×10^{19}	-	2.33×10^{19}	1.19×10^{21}	-
^{150}Nd→^{150}Sm	0.042	2.50×10^{19}	$\geq1.8\times10^{19}$ [68] $(1.7^{+1.1}_{-0.6})\times10^{19}$ [64] $(8.2\pm0.9)\times10^{18}$ [46]	2.63×10^{17}	1.66×10^{19}	6.7×10^{19} [63]
^{154}Sm→^{154}Gd	0.303	2.02×10^{21}	-	8.76×10^{20}	1.49×10^{22}	-
^{150}Gd→^{150}Dy	0.111	1.02×10^{21}	-	2.013×10^{20}	2.81×10^{21}	

was outlined in Section 3 of the present paper. Indeed, we showed that within the linearizing procedure framework, the pp interaction term does not contribute to the equations of motion if the condition of conserving the nucleon total number holds. However, in the mentioned papers the pp interaction influence on the phonon amplitudes is taken into account by averaging some specific double commutators on the vacuum state. Following the same path for the number non-conserving terms, their amplitudes in the phonon operator cannot be vanishing. According to Ref. [49], the experimental GT transition amplitude is reached for the pp interaction strength close to the $pnQRPA$ breaking down value. Moreover, the breaking down point of the fully renormalized $pnQRPA$ is lying close to and below the breaking down point of the standard $pnQRPA$. This result is on a par with our result from Ref. [11]. Therefore even if the ISR is satisfied, the principle problem of having a stable ground state for the mother and daughter nuclei still persists.

The attractive interaction of ph dipole-pairing type is responsible for the ground state correlations. To a less extent these are also caused by the $\mathcal{F}$ components of the new phonon operator. The projection of gauge is essential for restoring the ISR. The gauge projection of the $pnQRPA$ was previously achieved in Ref. [67] where the ISR is anyway satisfied within the unprojected picture. By contrast, therein the effect of projection is small.

Generally speaking, whenever some beauty conditions, like fully renormalization and gauge symmetry restoration, are met a certain tribute is expected to be payed. Thus, there are some specific weak points which require further improvements. Indeed, the average of the quasiparticle number operators has been approximately calculated. We feel that a better expression can be found for this quantity which is essential for the adopted iterative procedure. We hope that a better representation for the average number of quasiparticles will speed up the convergence of the iterative process. Moreover, this will allow us to extend our calculations to actinides region. The renormalized vacuum state is characterized by a non-vanishing average number of quasiparticles. That means that the $pnQRPA$ features are determined by the pairing properties not only through the occupation probabilities U^2 and V^2 but also by the averages of quasiparticle number operators. The question which arises is whether the $pnQRPA$ may influence the pairing properties. A positive answer could supply us with a unifying variational principle for both vacua, of quasiparticle and $pnQRPA$ boson respectively. This goal was in fact touched within a different context by Jolos *et al* [73]. These features concerning the description of the quasiparticle number operators in a better way as well as describing the BCS and the $pnQRPA$ in an unified fashion, by a set of coupled equations derived from a unique variational principle will be implemented in the near future.

Table 6.

The $\log ft$ values characterizing the β^+/EC and β^- processes associated to the intermediate odd-odd nuclei are listed.

Mother nucleus		odd-odd nucleus		Daughter nucleus
^{48}Ca	$\xleftarrow{\beta^+/EC}$	^{48}Sc	$\xrightarrow{\beta^-}$	^{48}Ti
Theor.	8.44		4.63	
^{76}Ge	$\xleftarrow{\beta^+/EC}$	^{76}As	$\xrightarrow{\beta^-}$	^{76}Se
Theor.	4.57		6.13	
^{82}Se	$\xleftarrow{\beta^+/EC}$	^{82}Br	$\xrightarrow{\beta^-}$	^{82}Kr
Theor.	8.11		7.18	
^{96}Zr	$\xleftarrow{\beta^+/EC}$	^{96}Nb	$\xrightarrow{\beta^-}$	^{96}Mo
Theor.	5.67		7.00	
^{100}Mo	$\xleftarrow{\beta^+/EC}$	^{100}Tc	$\xrightarrow{\beta^-}$	^{100}Ru
Exp.	$4.45^{+0.18}_{-0.30}$ [69]		4.66 [70]	
Theor.	4.65		4.1	
^{104}Ru	$\xleftarrow{\beta^+/EC}$	^{104}Rh	$\xrightarrow{\beta^-}$	^{104}Pd
Exp.	4.32 [61]		4.55 [61]	
Theor.	4.71		6.47	
^{110}Pd	$\xleftarrow{\beta^+/EC}$	^{110}Ag	$\xrightarrow{\beta^-}$	^{110}Cd
Exp.	4.08 [62]		4.66 [62]	
Theor.	4.14		6.32	
^{116}Cd	$\xleftarrow{\beta^+/EC}$	^{116}In	$\xrightarrow{\beta^-}$	^{116}Sn
Exp.	$4.45^{+0.18}_{-0.30}$ [71]		4.66 [72]	
Theor.	4.65		4.1	
^{128}Te	$\xleftarrow{\beta^+/EC}$	^{128}I	$\xrightarrow{\beta^-}$	^{128}Xe
Exp.	5.049 [65]		6.061 [66]	
Theor.	5.87		6.06	
^{130}Te	$\xleftarrow{\beta^+/EC}$	^{130}I	$\xrightarrow{\beta^-}$	^{130}Xe
Theor.	6.08		5.80	
^{148}Nd	$\xleftarrow{\beta^+/EC}$	^{148}Pm	$\xrightarrow{\beta^-}$	^{148}Sm
Theor.	6.8		7.33	
^{150}Nd	$\xleftarrow{\beta^+/EC}$	^{150}Pm	$\xrightarrow{\beta^-}$	^{150}Sm
Theor.	5.55		8.46	
^{154}Sm	$\xleftarrow{\beta^+/EC}$	^{154}Eu	$\xrightarrow{\beta^-}$	^{154}Gd
Theor.	5.52		5.13	
^{160}Gd	$\xleftarrow{\beta^+/EC}$	^{160}Tb	$\xrightarrow{\beta^-}$	^{160}Dy
Theor.	5.25		4.20	

6. CONCLUSIONS

Summarizing the results of this paper, one may say that restoring the gauge symmetry from the fully renormalized $pnQRPA$ provides a consistent and realistic description of the transition rate and, moreover, the ISR is obeyed. As shown in this paper, it seems that there is no need to include the pp interaction in the many body treatment of the process. Small deviations of the predicted and experimental GT resonance centroids suggest that the parameter χ should be fixed by fitting the centroids within the $GRFRpnQRPA$. By contrast to the standard $pnQRPA$ models where the strength of the pp interaction is not affecting the position of the GT resonance centroids, here the attractive interaction contributes to the distribution of the β^- strength. Therefore, the two strengths should be fixed at a time by fitting two data, either the GT resonance centroid and the $\log\ ft$ value of one decay of the intermediate odd-odd nuclei or by fixing the $\log\ ft$ values corresponding to the single beta decays of the odd-odd intermediate nucleus.

Before closing let us enumerate the results of our numerical analysis.

- Results for the summed strength $B(GT^-)$ agree quite well with the existent experimental data. Also the summed $B(GT^+)$ strengths for ^{76}Ti and ^{76}Se agree reasonable well with the corresponding experimental data.
- The GT resonance centroid locations as well as the total strength of the GT resonance for ^{100}Tc and ^{116}In are quite well described.
- The calculated half-lives are in good agreement with the experimental data.

The gauge projection of the $pnQRPA$ was previously achieved in Ref. [67] where the ISR is anyway satisfied within the unprojected picture. By contrast therein the effect of projection is small.

Concluding, the present calculations prove that the $GRFRpnQRPA$ is able to describe in a realistic manner the $2\nu\beta\beta$ decay and moreover satisfies the ISR.

Acknowledgments. This paper was written in the Honor of my PhD supervisor, Prof. A. Sandulescu, on the occasion of his 80th anniversary. I wish him a long live and to keep his high enthusiasm for whatever is he doing.

This work was partially supported by the Romanian Ministry for Education Research Youth and Sport through the CNCSIS project ID-2/5.10.2011.

7. APPENDIX A

The sub-matrices involved in the *GRFRpnQRPA* equations are given by the following expressions:

$$\begin{aligned}
(A_{11})_{p_1n_1;pn} &= E^{ren}(pn)\delta_{pn;p_1n_1} + 2\chi\sigma^{(1)T}_{p_1n_1;pn},\\
(A_{12})_{p_1n_1;pn} &= 0 = (A_{21})_{p_1n_1;pn},\\
(B_{12})_{p_1n_1;pn} &= 2\chi\sigma^{(1)T}_{p_1n_1;pn} = (B_{21})_{p_1n_1;pn},\\
(B_{11})_{p_1n_1;pn} &= 0 = (B_{22})_{p_1n_1;pn},\\
(A_{22})_{p_1n_1;pn} &= |E^{ren}(pn)|\delta_{pn;p_1n_1} + 2\chi\sigma^{(1)T}_{p_1n_1;pn}.
\end{aligned} \tag{35}$$

REFERENCES

1. H. Primakof, S. Rosen, Rep. Prog. Phys. **22**, 125 (1959).
2. W. C. Haxton, G. J. Stephenson, Jr. Prog. Part. Nucl. Phys. **12**, 409 (1984).
3. J. D. Vergados, Phys. Rep. **361**, 1 (2001).
4. J. Suhonen and O. Civitarese, Phys. Rep. **300**, 123 (1998).
5. T. Tomoda, Re. Prog. Phys. **54**, 53 (1991).
6. A. Faessler, Prog. Part. Nucl. Phys. **21**, 183 (1988).
7. A. A. Raduta, Prog. Part. Nucl. Phys. **48**, 233 (2002).
8. A. A. Raduta, A.Faessler, S. Stoica, Nucl. Phys. **A534**, 149 (1991).
9. A. A. Raduta, A. Faessler, S. Stoica, W. Kaminsky, Phys. Lett. **254**, 7 (1991).
10. J. Toivanen and J. Suhonen,Phys. Rev. Lett. **75**, 410 (1995).
11. A. A. Raduta, C. M. Raduta, W. Kaminski, A. Faessler, Nucl. Phys. A **634**, 497 (1998).
12. A. A. Raduta, C. M. Raduta, B. Codirla, Nucl. Phys. A **678**, 382 (2000).
13. A. A. Raduta, F. Simkovich, A. Faessler, Jour. Phys. G **26**, 793 (2000).
14. C. M. Raduta and A. A. Raduta, Nucl. Phys. A **756**, 153 (2005).
15. C. M. Raduta and A. A. Raduta, Phys. Rev. C **82**, 068501 (2010).
16. C. M. Raduta and A. A. Raduta, J. Phys. G; Nucl. Part. Physics **38**, 055102 (2011).
17. A. A. Raduta, D. S. Delion, N. Lo Iudice, Nucl. Phys. A **564**, 185 (1993).
18. A. A. Raduta, A. Escuderos, A. Faessler, E. Moya de Guerra, P. Sarriguren, Phys. Rev. C **69**, 064321 (2004).
19. A. A. Raduta, C. M. Raduta and A. Escuderos, Phys. Rev. C **71**, 164 (2005).
20. A. A. Raduta, N. Lo Iudice, I. I. Ursu, Nucl. Phys. A **584**, 84 (1995).
21. A. A. Raduta, A. Escuderos, E. Moya de Guerra, Phys. Rev. C **65**, 024312 (2002).
22. A. A. Raduta, A. Faessler, D. S. Delion, Nucl. Phys. A **564**, 185 (1993); Phys. Lett. B **312**, 13 (1993).
23. A. A. Raduta, D. S. Delion, A. Faessler, Nucl. Phys. A **617**, 176 (1997).
24. S. G. Nilsson, Mat. Fys. Medd. K. Dan. Vid. Selsk. **29** no. 16 (1955).
25. M. E. Rose, *Elementary Theory of Angular Momentum* (Wiley, New York, 1957).
26. H. Homma *et al.*, Phys. Rev. C **54**, 2972 (1996).
27. A. Balysh *et al.*, Phys. Rev. Lett. **77**, 5186 (1996).
28. F. T. Avignone III *et al.*, Phys. Lett. B **256**, 559 (1991).

29. S. R. Elliot, A. A. Hahn, M. K. Moe, Phys. Rev. Lett.**59**, 2020 (1987).
30. S. R. Elliot and P. Vogel, Ann. Rev. Nucl. Part. Sci. **52**, 115 (2002); A. S. Barabasch, Czech. J. Phys. **52**, 567 (2002).
31. H. Ejiri *et al.*, Phys. Lett. B **258**, 17 (1991).
32. T. Kirsten *et al.*, in *Proceedings of the International Symposium on Nuclear Beta Decays and Neutrino*, T. Kotani, H. Ejiri, E. Takasugi (eds.), p. 81 (Singapore, World Scientific, 1986).
33. S. I. Vasil'ev *et al.*, JETP Lett. **51**, 622 (1990).
34. K.Grotz and H. V. Klapdor, Phys. Lett. B **157**, 242 (1985).
35. M. Hirsch *et al.*, Phys. Rep. **242**, 403 (1994).
36. X. R. Wu *et al.*, Commun. Theor. Phys. **20**, 453 (1993).
37. L.Zamick, N. Auerbach, Phys. Rev. C **26**, 2185 (1982).
38. K. Yako, *et al.*, Phys. Rev. Lett. **103**, 012503.m (2009).
39. B. D. Anderson *et al.*,Phys. Rev. C **31**, 1161 (1985).
40. W. P. Alford, *et al.*, Nucl. Phys. A **514**, 49 (1990).
41. R. Madey *et al.*, Phys. Rev. C **40**, 540 (1989).
42. R. Helmer *et al.*, Phys. Rev. C **55**, 2802 (1997).
43. E.-W. Grewe *et al.*, Phys. Rev. C **76**, 054307 (2007).
44. E.-W Grewe *et al.*, Phys. Rev. C **78**, 044301 (2008).
45. H. Dohmann *et al.*, Phys. Rev. C **78**, 0411602(R) (2008).
46. A. S. Barabash, Phys. Rev. C **81**, 035501 (2010).
47. H. Akimune *et al.*, Phys. Lett. B **394**, 23 (1997).
48. Vadim Rodin, Amand Faessler, Phys. Rev. C **66**, 051303(R) (2002).
49. L. Pacearescu, V. Rodin, F. Simkovic, Amand Faessler, Phys. Rev. C **68**, 064310 (2003).
50. O. Civitarese, Reboiro, Phys. Rev. C **71**, 014318 (2005).
51. K. Hara, Prog. Theor. Phys. **32**, 88 (1964).
52. K. Ikeda, Prog. Theor. Phys. **31**, 434 (1964); K. Ikeda, T. Udagawa, M. Yamamura, Prog. Theor. Phys. **33**, 22 (1965).
53. W. Thomas, Naturwissenschaften **13**, 627 (1925); W. Kuhn, Z. Phys. **33**, 408 (1925); F. Reiche and W. Thomas, Z. Phys. **34**, 510 (1925).
54. E. W. Hennecke, O. K. Manuel, D. D. Sabu, Phys. Rev. C **11**, 1378 (1975).
55. J. Lin *et al.*, Nucl. Phys. A **481**, 477 (1988).
56. H. V. Klapdor, K. Grotz, Phys. Lett. **142**, 323 (1984).
57. M. Aunola, J. Suhonen, Nucl. Phys. A **602**, 133 (1996).
58. D. Cha, Phys. Rev. **27**, 2269 (1987).
59. J. Suhonen, O. Civitarese, Phys. Rev. C **49**, 3055 (1994).
60. M. Hirsch, X. R. Wu, H. V. Klapdor-Kleingrothaus, Ching Cheng-rui, Ho Tso-hsui, Phys. Rep. **242**, 403 (1994).
61. Jean Blachot, Nuclear Data Sheets **92**, 455 (2001).
62. D. De Frenne, E. Jacobs, Nuclear Data Sheets **89**, 481 (2000).
63. J. G. Hirsch, O. Castanos, P. O. Hess, O. Civitarese, Nucl. Phys. A **589**, 445 (1995).
64. C. Arpesella *et al.*, Europhys. Lett. **27**, 29 (1994).
65. C. M. Lederer, V. S. Shirley, *Table of Isotopes*, p. 631 (7th edn., Wiley, New York, 1978).
66. M. Kanbe, K. Kitao, Nucl. Data Sheets **94**, 227 (2001).
67. O. Civitarese *et al.*, Nucl. Phys. A **524**, 404 (1991).
68. A. L. Klimenko *et al.*, Nucl. Instrum. Methods, Phys. Rev. B **16**, 446 (1986).

69. A. Garcia *et al.*, Phys. Rev. C **47**, 2910 (1993).
70. Balraj Sinh, Nuclear Data Sheets **81**, 1 (1997).
71. M. Battacharya *et al.*, Phys. Rev. C **58**, 1247 (1998).
72. Jean Bachot, Nuclear Data Sheets **92**, 227 (2001).
73. R. V. Jolos, W. Rybarska-Nawrocka, Zeit.f. Physik A **296**, 73 (1980).